

ROBOTIC TANKETTE FOR INTELLIGENT BIOENERGY AGRICULTURE: DESIGN, DEVELOPMENT AND FIELD TESTS¹

MARCO F. S. XAUD*, ANTONIO C. LEITE†, EVELYN S. BARBOSA^{2*}, HENRIQUE D. FARIA^{2*}, GABRIEL S. M. LOUREIRO^{2*}, PÅL J. FROM*

**Norwegian University of Life Sciences,
Faculty of Science and Technology,
P.O. Box 5003, NO-1432, Ås, Norway.*

*†Pontifical Catholic University of Rio de Janeiro,
Department of Electrical Engineering,
Postal code 22451-900 Rio de Janeiro RJ, Brazil.*

mafernan@nmbu.no, antonio@ele.puc-rio.br, evelynsoaresb@poli.ufrj.br,
hd.faria@poli.ufrj.br, gloureiro@poli.ufrj.br, pal.johan.from@nmbu.no

Abstract— In recent years, the use of robots in agriculture has been increasing mainly due to the high demand of productivity, precision and efficiency, which follow the climate change effects and world population growth. Unlike conventional agriculture, sugarcane farms are usually regions with dense vegetation, gigantic areas, and subjected to extreme weather conditions, such as intense heat, moisture and rain. TIBA - Tankette for Intelligent BioEnergy Agriculture - is the first result of an R&D project which strives to develop an autonomous mobile robotic system for carrying out a number of agricultural tasks in sugarcane fields. The proposed concept consists of a semi-autonomous, low-cost, dust and waterproof tankette-type vehicle, capable of infiltrating dense vegetation in plantation tunnels and carry several sensing systems, in order to perform mapping of hard-to-access areas and collecting samples. This paper presents an overview of the robot mechanical design, the embedded electronics and software architecture, and the construction of a first prototype. Preliminary results obtained in field tests validate the proposed conceptual design and bring about several challenges and potential applications for robot autonomous navigation, as well as to build a new prototype with additional functionality.

Keywords— Mobile robots, Agricultural robotics, Embedded electronics, Sensors Integration.

Resumo— Nos últimos anos, o uso de sistemas robóticos na agricultura tem aumentado principalmente devido à alta demanda em termos de produtividade, precisão e eficiência, causadas pelos efeitos das mudanças climáticas e pelo crescimento da população mundial. Ao contrário da agricultura convencional, fazendas de cana de açúcar são geralmente regiões com densa vegetação, áreas gigantescas, e sujeitas a condições meteorológicas extremas, como calor, umidade e chuva intensa. TIBA - *Tankette for Intelligent BioEnergy Agriculture* - é o resultado preliminar de um projeto de P&D cujo objetivo é desenvolver um sistema robótico móvel e autônomo capaz de realizar diversas tarefas agrícolas em fazendas de cana-de-açúcar. O conceito proposto consiste de um pequeno veículo tipo tanque, de baixo custo, à prova de poeira e água, capaz de se infiltrar em densas vegetações em túneis de plantação, carregando diversos sensores e dispositivos para realizar tarefas de mapeamento em áreas de difícil acesso e coleta de amostras. Este trabalho apresenta uma visão geral do projeto mecânico do robô, uma descrição da arquitetura de software e eletrônica embarcada e a construção de um primeiro protótipo. Resultados preliminares obtidos em testes de campo validam o projeto conceitual proposto e levantam vários desafios e potenciais aplicações para navegação autônoma do robô bem como para construir um novo protótipo com funcionalidades adicionais.

Palavras-chave— Robôs móveis, Robótica agrícola, Eletrônica embarcada, Integração de sensores.

1 Introduction

In recent years, the use of robots in agriculture or “agbots” has been growing significantly due to the high demand for increased productivity and precision, which was brought about by climate changes and their effects on the environment (Billingsley et al., 2008). Moreover, the growth of the world’s population has motivated farmers to seek an increase in the efficiency of food production, for instance, reducing the waste of inputs and increasing the productivity of small cultivated areas, at

the lowest possible cost (Edan et al., 2009). Currently, there are more than 50 different types of mobile robots in the world deployed for agricultural purposes. These robots, in general, have specialized accessories, tools and arms to perform a wide range of agricultural tasks (Bechar and Vigneault, 2017; Grimstad and From, 2017). This number gives us an idea of how the potential of robotic technology is embedded in agricultural systems. Following this trend, it is possible to find devices vacuuming apples off the trees in the US, octopus-like robots for collecting strawberries in Spain, and machines feeding and milking cows in the UK. These are just a few examples of how robots are taking over fields around the world. These concerns about food production do not belong exclusively to Europe and can also be considered in many countries of Central

¹This work was partially supported by the UTFORSK Partnership Programme from The Norwegian Centre for International Cooperation in Education (SIU), project number UTF-2016-long-term/10097.

²Visiting Research Student at the Norwegian University of Life Sciences.

and South America, particularly, in Brazil. Although, the Brazilian agricultural industry has a high degree of automation for the planting and harvesting of grains and sugarcane in large areas, farmers still do not use autonomous robotic systems to perform basic and complex agricultural tasks in small areas, such as, vegetable gardens and orchards. Some basic agricultural tasks include sowing, fertilizing, and irrigation, while some complex agricultural tasks consist of harvesting fruits, killing weeds and plant phenotyping (Bac et al., 2014; Midtiby et al., 2016; Li et al., 2014).

Sugarcane has emerged as an important alternative to fossil fuels since, besides to produce sugar, it can be used as a clean, renewable source of energy reducing the petroleum use - and consequently greenhouse gas emissions - and also to generate other useful products such as, bioelectricity and bioplastics (Davis et al., 2009). Sugarcane farms usually need gigantic areas for planting, which requires many employees and machinery, as well as high costs for maintenance and logistics. Moreover, most of sugarcane tasks are laborious and tedious, susceptible to human errors and performed in a harsh environment subject to bad weather conditions, dense vegetation, and wild life. Some of the relevant tasks include: cataloging of plants, identification of weeds/pests and misplanting (empty spots), classification of soil types, and evaluation of plant health.

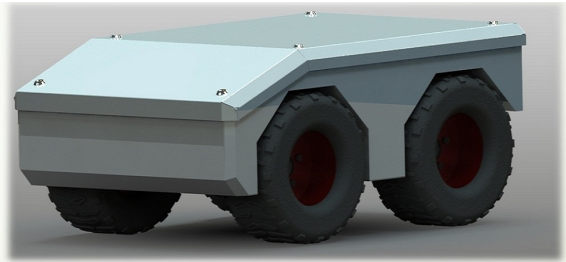


Figure 1: Conceptual design of the TIBA robot.

Following this motivation, in this proposal we aim to develop the conceptual design and build the prototype of a mobile robot to perform autonomous tasks of mapping difficult-to-access areas and collecting soil samples in sugarcane farms. TIBA - Tankette for Intelligent BioEnergy Agriculture - is an alternative solution to deploying several robot units in a swarm-based approach to cover a wide area, reducing or eliminating the employment of man-power under unhealthy environments and enhancing the farm logistics. To the best of our knowledge, TIBA (Fig. 1) is the first prototype of a 4-wheeled mobile robot to be developed to carry out precision agricultural tasks on sugarcane plantations. Similar systems have been tested in vineyards, orchards and corn production

in the US (e.g., Rowbot).

2 Robot for Sugarcane Fields

In this section, we describe the main aspects of the proposed conceptual design of the TIBA robot in terms of mechanical structure, locomotion system, embedded electronics, and software architecture. This design was conceived based on the main challenges found in sugarcane fields, such as tight and dense plant rows, soil mostly composed of sand (66.7%) and clay/mud (33.3%), and possibility of plant leaves getting trapped in the robot parts.

2.1 Mechanical Design

The mechanical structure was designed to provide a very compact solution yet capable to yield 3 degrees-of-freedom, translation x, y and the rotation θ . The robot is a 4-wheeled small tank composed of a 3 mm thick steel chassis and 1.5 mm aluminum walls (Fig.1). There is also an aluminum lid on the top, in order to cover the robot interior, protect it against water and dust - which is also provided by rubber tapes along the lid perimeter - and accommodate sensors or other devices over its surface, such as laser scanners, solar panels, etc. The robot carcass has also customized holes to provide mechanical accommodation and view of sensors and cameras to the outside. The robot interior accommodates the mechanical arrangement—composed of two motors, two gearboxes, belts/chains, pulleys/sprockets, wheel bearings and adapters—and the support for the electronics system, which is composed of aluminum profiles in such an arrangement that does not interfere with the mechanical components.

The main motivation for this project was the reduction of costs. Thus, a driving configuration that provides the best mobility with the lowest number of motors and other mechanical parts had to be chosen. The skid-steering configuration, as shown in Fig. 2(a), was selected as a suitable and low-cost solution, which only demands the employment of two motors, being the curved movements achieved by applying differential speeds in each side. In addition, the trajectory control of skid-steering robots is already established in the literature, and its implementation can be based on several recent works, such as (Tchoñ et al., 2015). In TIBA, one motor is designated to drive the two wheels of the same side, as shown in Fig. 2(b). Those wheels are connected by a belt, which provides the same rotation rate to them. Finally, one gearbox connect to each motor provides the torque increase and speed reduction. A right-angle gearbox model was employed as a solution for the confined space.

Aiming to sustain the cost reduction strategy, the manufacturer and models of the motors, gear-

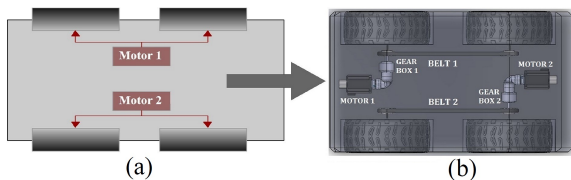


Figure 2: Driving configuration - (a) skid-steering; (b) TIBA mechanical arrangement.

boxes and wheels were selected from the set employed in the existing robot Thorvald II (Grimstad and From, 2017), so as to get out of their already verified advantages, which include reliability, low-cost, robustness, easiness for prototyping, and compatibility with other components. The wheels are a customized set of tire and rim suitable for snow, sand and clay terrain. To define the suitable set of motors and gearboxes, a calculation of the needed torque had to be performed. Given the selected wheel model - with $r_w = 20\text{ cm}$ tire radius - and the required operational terrain - clay and sand - we could estimate the necessary linear force to overcome the static friction between the tire rubber and the ground.

By considering an estimated robot weight of $M \approx 130\text{ kg}$, the Coulomb friction coefficient and the rolling resistance coefficient between an off-road tire and sand of $\mu_s = 0.6$ and $C_{rrs} = 0.2$ respectively, and the same coefficients for wet earth road or clay of $\mu_c = 0.55$ and $C_{rrc} = 0.08$ (Wong, 2008), the necessary force to overcome the friction applied in each wheel is given by $F_w = N_w \mu_s$, where N_w is the normal force on each wheel, and μ_s is the taken as the worst case among the terrain possibilities. By considering $g \approx 9.8\text{ m/s}^2$, the normal force is approximately given by $N_w = Mg/4 = 130 \times 9.8/4 = 318.5\text{ N}$, and hence, $F_w = 318.5 \times 0.6 = 191.1\text{ N}$. The necessary torque τ_w on each wheel is given by $\tau_w = F_w r_w$, which yields $\tau_w = 191.1 \times 0.2 = 38.22\text{ N.m}$. Finally since each motor drives two wheels at the same time and considering that this torque is equally distributed between them along the belt, the necessary torque to drive each wheel/belt set is given by $\bar{\tau}_b = 76.44\text{ N.m}$.

Among the available motor options from the selected manufacturer, the model 3MeN[®] BL840 provides the higher nominal torque of $\tau_m = 16\text{ kgf.cm} \approx 1.57\text{ N.m}$. Given that, among the available gearbox options from the selected manufacturer, the model APEX[®] AER070-050 provides a reduction ratio of 50:1. This drives the wheel/belt set with an increased torque of $\tau_b = 50 \times \tau_m = 78.50\text{ N.m}$, which is more than the needed value $\bar{\tau}_b$, as calculated previously.

Without any load, this motor/gearbox combination provides an output angular speed of 3000 rpm in the input of each gearbox set, and

an output angular speed of $3000/50 = 60\text{ rpm}$ in each wheel, which provides a total linear speed of $v = 2\pi \times 60 \times 0.2/60 \approx 1.26\text{ m/s}$ or $v \approx 4.52\text{ km/h}$. Considering the given environment and operational requirements for the robot, this is a fairly fast and safe maximum speed.

2.2 Embedded Electronics Design

The embedded electronics architecture of the robot was also designed so as to comply with the cost and environment requirements, and thus several electronic parts from the robot Thorvald II were used, such as the motor, power driver, mechanical relays, computer, rugged cable/connectors, and DIN rail (Fig. 3).



Figure 3: Embedded electronics parts - (a) Motor; (b) NUC computer; (c) DIN rail arrangements; (d) battery pack; (e) joystick; (f) motor driver.

The power is supplied by one 48VDC NiMH Battery Pack, and distributed into two power buses of 48VDC and 12VDC. The former feeds the power controller driver, and the latter supplies the computer, peripheral sensors, and a *Vehicle Support System* (VSS) - which is represented in the first version by an Arduino board. The computer Intel[®] NUC NUC6I5SYK Skylake gives a compact, lightweight and practical solution for a first prototype, and counts with a fairly powerful processor Intel Core i5 and several USB ports. The driver Robotek[®] FBL2360 is also a compact solution with two channels, which allow the control of two different motors in the same device. The control signals are communicated from the PC to the driver via *Controller Area Network* (CAN), which is an established and robust network for sensors and actuators communication with strict error detection. A set of DC-DC converters, low-power relays and a Gigabit Ethernet switch gives the functionality of adding/removing any peripheral device or sensor from the system, communicate them to the computer, and turn them on/off individually to save energy.

The VSS has the role of this relay activation, reading voltage and current measurements, and communicate them to the PC via CAN. The VSS

is also integrated with sensors for the electronics system self-monitoring, such as the internal temperature and humidity. The system also counts a touchscreen panel mounted on back of the robot, and an XBox wireless joystick for the control in manual mode. The panel and the joystick antenna are both connected to the PC directly via USB, being the cables routed outside the robot through a waterproof connector. All the electronic devices were mounted over a robust and firm aluminum structure. The DIN-rail was a robust solution for wiring and keeps the connections firm under vibration and impact conditions.

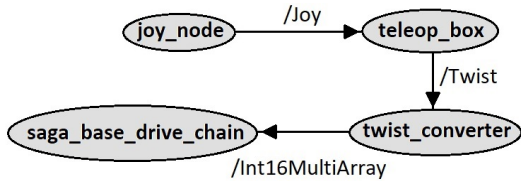


Figure 4: Diagram of ROS nodes.

2.3 Software Architecture

The robot software is developed on the modular multi-threaded control framework ROS (Quigley et al., 2009), which presents a large community with continuous expansion of software modules (Fig. 4). The prototype is teleoperated using a Xbox One wireless joystick. The teleop_box node is responsible to map the joystick axis and buttons to the desired velocities and gains. The velocities can be modeled as an increment of velocities on the xy axis. Then, a twist message is published on a topic. The twist converter node subscribed to the Twist topic and calculates the real velocities values. Then, it publishes them on a topic that the saga_base_drive_chain node is subscribed. Finally, the latter is responsible to communicate with the drivers via the CANopen protocol.

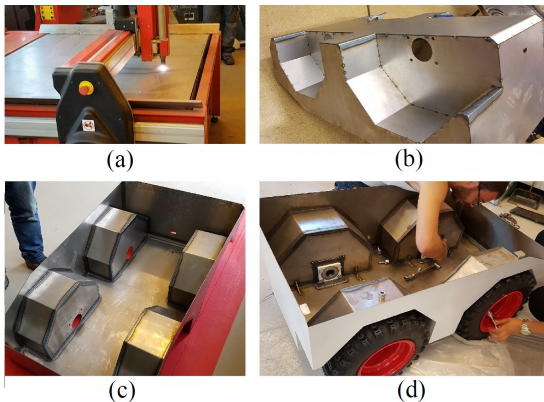


Figure 5: Assembly of early prototype - (a) cutting of steel and aluminum plates by using plasma cutter; (b) welded parts; (c) chassis and carcass; (d) assembly of mechanics system.

2.4 First Robot Prototype

The first prototype, shown in Figures 5 and 6, was constructed in order to validate all the proposed mechanical concepts, feasibility of the implemented skid-steering configuration, robot behaviour in the expected terrains, and robustness of the embedded electronics system to vibration and environmental conditions. The robot chassis and carcass were basically a welded assembly of cut and bent metal sheets. Only for this first version, some modifications and simplifications were implemented due to cost reductions, delays in delivery of equipment and assembly pieces, and fulfillment of schedules.

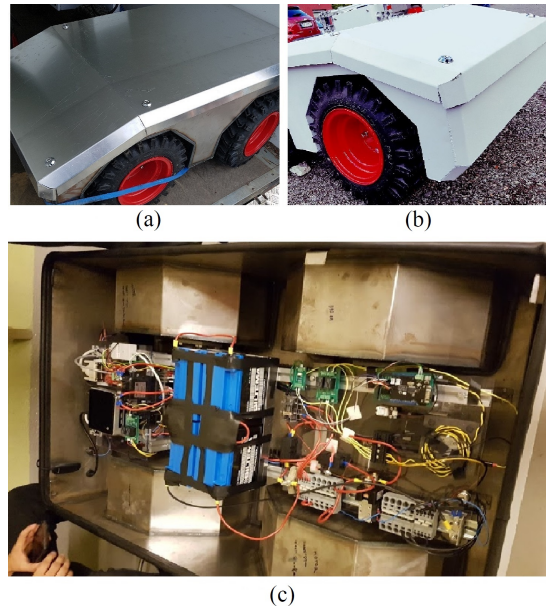


Figure 6: Early prototype - (a) top lid and robot closed; (b) painted prototype; (c) compact electronics system on the support.

Among the most significant simplifications, the robot mechanical structure, except the top lid, was made entirely of steel, so that the parts welding could be performed faster. The desired wheel bearing model could not be found on time and, thus, an alternative one from Volvo was used, which was however heavier, and needed several mechanical adapters for fixation. The belts and pulleys were replaced by chains and sprockets, since the belts would demand a very large width for the given torque/power and, hence, the redesign of the electronics support structure. Finally, due to the lack of available encoders, the motor control and odometry were implemented by only using the motors hall-effect sensors. This condition restricted and hindered the motor position control and high accuracy for an odometry model, but it was satisfactory for the first tests.

3 Field Tests

The first field tests were performed at the UMOE BioEnergy sugarcane farm, at Presidente Prudente, in the state of São Paulo, Brazil. The main motivations for the farm visit and the robot tests were: evaluation of the mechanical concept and proposed dimensions, better examination and learning of the environment, and investigation of future modifications and new features, as shown in Fig. 7a. A few sensors were initially employed in this field test, so that the understanding of the environment could be quantified in several data to be later analyzed and used to help the investigation of methods for the robot navigation, as shown in Figures 7b and 7c.

The tests were performed in different rounds, being all the sensor data of each round recorded in a different `.bag` file in the ROS environment. For this test, different chains/sprocket configurations were tested, as shown in Fig. 7d.

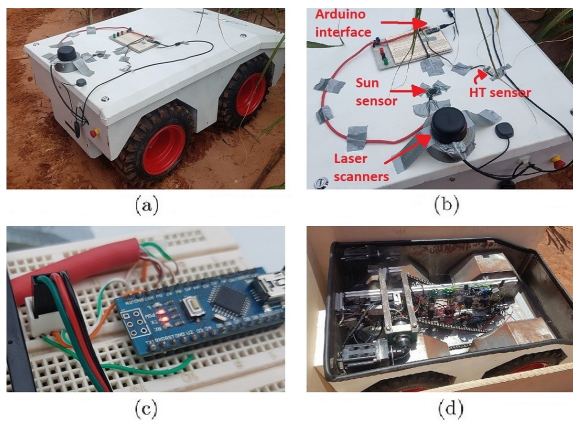


Figure 7: Preparation of robot for field test - (a) robot in the field; (b) sensors attached *ad hoc* to the top lid; (c) interface for connecting solar sensor and HT sensor to Arduino; (d) electro-mechanical arrangement for the test.

3.1 Mechanical Concept Evaluation

The robot presented a fairly satisfactory performance for remote navigation over the sugarcane operational terrain, composed of sand and clay. As expected, its behavior was rough for operations in concrete and asphalt, because the skid-steering driving configuration and the selected wheel type require that the tire slides over the terrain, as shown in Fig. 8a. The structure proved to be robust to the uneven terrain, and had a remarkable performance for unexpected crevices on the soil, as shown in Figures 8b and 8c, which have been formed due to the accumulation of rain water in that period.

The skid-steering arrangement showed to be very convenient to achieve the desired motion

and degrees-of-freedom: forward, backwards, rotation around own axis, and curves. The infiltration through the sugarcane tunnels was tested for plants with approximately 1, 2 and 3 meters high (Fig. 9). For the first two cases, the robot was able to travel along the tunnel without any obstacle for its motion. In the 3 meters high case, were the plants are tall enough to fall back towards the tunnel center and create soft obstacles, there were some points in which the robot width seemed to be wide for this tightness and got the risk to collide with the plant stems. For all the cases, it was not observed the occurrence of plant leaves trapping or getting stuck to the structure or the wheels.

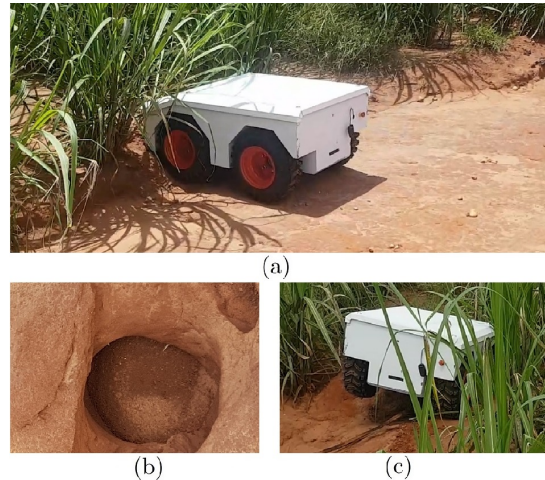


Figure 8: Field test in the UMOE BioEnergy farm, Presidente Prudente, Brazil - (a) robot entering the tunnel; (b) uneven terrain and big crevices; (c) robot passing over crevice, the structure is tilted and struggles to overcome the valley.



Figure 9: Field test in UMOE Bioenergy farm, Presidente Prudente SP, Brazil - Tunnels of plants.

3.2 Thermal Mapping

A FLIR® One V2 infrared camera in a smartphone was attached to the robot hood in order to capture thermal images and videos of the sugarcane tunnel environment. This was firstly proposed as a cheap and efficient solution for the robot navigation, which was already proposed and implemented in many recent works, as by (Fehlman and Hinders, 2009).

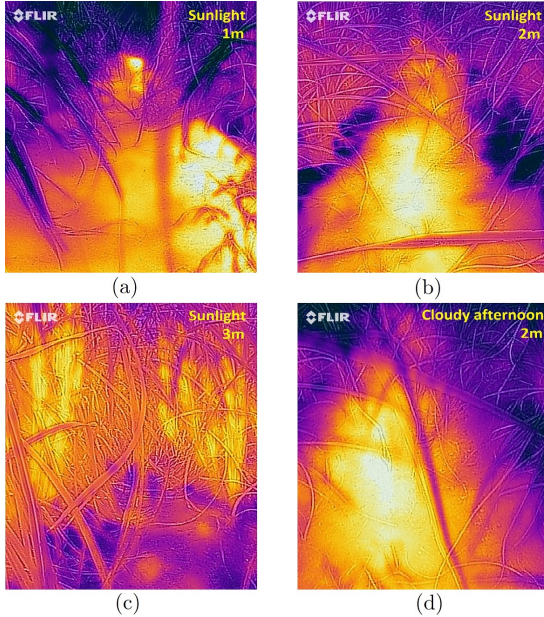


Figure 10: Thermal map - (a) sunlight, 1 m plants; (b) sunlight, 2 m plants; (c) sunlight, 3 m plants; (d) late afternoon, cloudy, 2 m plants.

The test was applied for rides through sugarcanes with approximately 1, 2 and 3 meters of height, and during the sunlight period - around 3 p.m. - and in the late afternoon - around 6 p.m. and cloudy. The collected data were greatly satisfactory. The results for the sunlight period (Fig. 10) show that the thermal mapping creates a path along the ground due to the temperature difference between the land and the plants. If compared to the image of a regular HD camera, the thermal path is much more distinguishable, and remains clear even when plants are trapping in front of the camera. For 1 and 2 meters tall plants, the ground is much warmer than the sugarcane, and a cold kerb is also created at the path border, since the base of plantation is even colder. For 3 meters tall plants, the sunlight does not reach the ground strongly. Therefore, the thermal map shows that the ground is colder than the plants and no kerb is visible. However, even with a smaller temperature difference, the created path is strong enough to be distinguished.

The results for a cloudy afternoon, as shown in Fig. 10d, and 2 meters tall plants show that the heat pattern held strongly, so that clear paths

were still visible. This was valid for all the three plant heights. Even though the thermal mapping were not also performed in rainy conditions, the collected results were greatly satisfactory, since navigation by using a small thermal camera would be a suitable low-cost solution, which is one of the robot concept pillars. In addition to the taken thermal images and videos taken from the forward view, some media was also collected with the camera slightly turned to the sides. The data can be used as an input for image processing and detection of the corridor centerline to be followed by the robot. Several techniques could be employed for that, such as simple and low-cost ones (e.g., color threshold), as shown in Fig. 11, or complex ones (e.g., training artificial neural network for image classification).

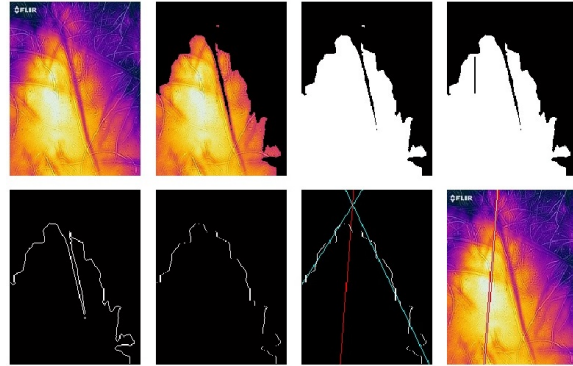


Figure 11: Example of thermal image processing performed with the collected data from the field test (the centerline is defined by linear regression of the margins of *warm* and orange triangle output from a color threshold filter).

3.3 Odometry and Laser Scanner

A 3D environment of the robot model and motion was created in ROS by using the robot odometry. In this model, the robot position, orientation, linear and angular speeds are calculated from the motors odometry. Typically, the data from both encoders and a hall effect sensor are used, but the current prototype still carries only the hall effect sensors due to device delivery delays. The precision obtained by the hall sensor effect was considered satisfactory for the implementation of the first 3D model. The goal of the 3D environment is to make possible the simulation of the robot motion, the visualization of sensor collected data - depending on the used platform - and hence the investigation of different techniques for the robot navigation and autonomy.

For this prototype, the data of two laser scanners attached to the robot top lid - LIDAR® A2 and Hokuyo® - were collected and viewed in the 3D environment together with the robot model

(Fig. 12). Notice in Figure 13 that an interesting corridor of points was observed with the visualization of the Hokuyo laser data, which is the scanning of the existing plant corridor deployed along the sugarcane tunnel. Even though the precision of those laser scanners may not be the most recommended for this application - due to the high density of sugarcanes in such an environment - the observed data clearly motivates the use of those devices to aid in a future robot mapping system.

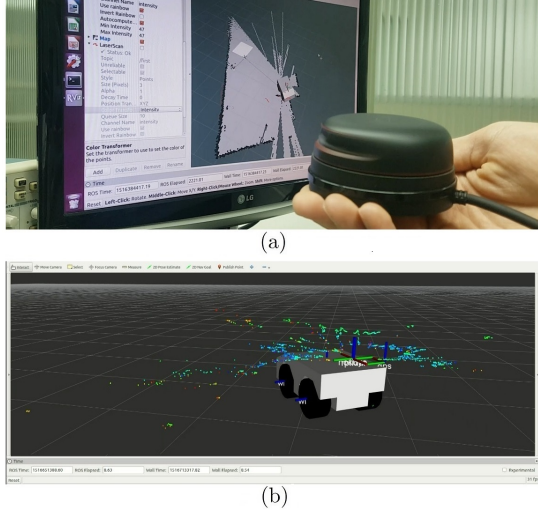


Figure 12: Laser data and 3D environment mapping - (a) LIDAR; (b) Hokuyo.

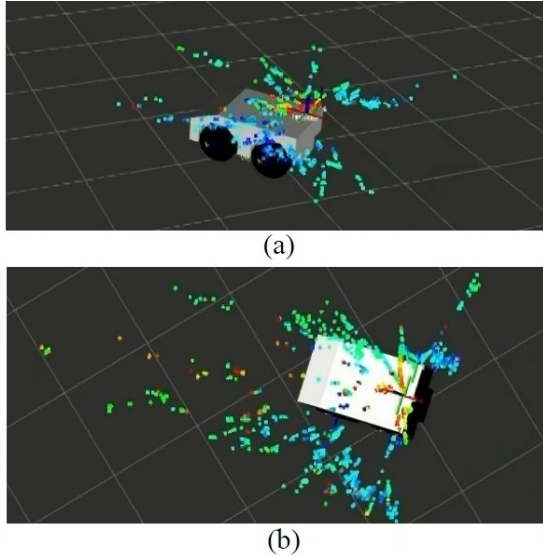


Figure 13: Corridor of points formed due to the existing corridor of plants (sugarcane tunnel) - (a) perspective view; (b) top view.

3.4 Solar Sensor

One Solar Mems[®] NANO-ISSX-60 sun sensor was attached to the robot top lid in order to detect the direction of the sunlight (Fig. 14). The sensor

power and signals were connected directly to the Arduino, and them communicated to the robot computer via CAN network. Solar sensors consist of a simple embedded technology that make possible the calculation of the sun ray incident vector given its projection angles along orthogonal axes. The sunlight is detected by a quadrant photodetector device aligned to the x - and y -axes, from where four voltage levels denoted by V_1 , V_2 , V_3 , V_4 are promptly read. The projection angles α_x and α_y are hence given by:

$$\alpha_x = \tan^{-1}(C F_x), \quad \alpha_y = \tan^{-1}(C F_y), \quad (1)$$

where

$$F_x = \frac{V_1 + V_2 - V_3 - V_4}{V_1 + V_2 + V_3 + V_4}, \quad (2)$$

$$F_y = \frac{V_2 + V_3 - V_1 - V_4}{V_1 + V_2 + V_3 + V_4}, \quad (3)$$

and C is a parameter that depends on the selected sensor model (SolarMEMS, 2017).

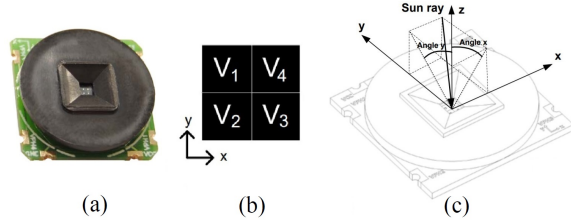


Figure 14: (a) Sensor NANO-ISSX; (b) photodetector cells; (c) sunlight projections along axes.

The use of solar sensors in the first tests was initially motivated by their low-cost, simplicity for installation, and some important works that employed them for research with odometry (Lambert et al., 2011), attitude control (Ortega et al., 2010), and navigation (Volpe, 1999). For this robot, the main motivation was to test the device in the sugarcane environment and track the behaviour of the collected result in both sunny and cloudy weather conditions and uneven terrain, which can cause a considerable disturbance in the expected results. One of the test goals is to determine the feasibility of using solar sensors to aid the robot initial heading for navigation. Another goal is related to a possible future improvement for this robot, which is the use of solar panels for the power supply. The solar sensor may help to control them to an efficient orientation configuration that can get the most out of the present sunlight.

3.5 Temperature and Humidity Sensor

A temperature and relative air humidity (HT) sensor - model RHT03 - was attached to the robot top lid, and electrically connected to the Arduino.

HT sensors are strongly used in self-monitoring of embedded electronics systems against overheat and corrosion due to sea air. Their use was motivated for our environment, since it is subjected to high temperatures and humidity due to the rain. Future implementations may be motivated by the use two HT sensors: one within the chassis for the electronics self-monitoring, and another on the robot surface for the environment monitoring.

4 Concluding Remarks and Perspectives

The designed robot showed to be an efficient low-cost solution for deployment in gigantic sugarcane fields, with good motivation for operation in swarm-based approach. Since the conceptual test phase of the robot design was concluded and the collected data was analyzed, some future developments should be implemented.

4.1 Mechanical Modifications

Although the mechanical concept presented a good performance, the wheel fixation to the robot chassis is worryingly stiff, while the chassis by itself is worryingly flexible. A proposed modification for the next robot version is to utilize steering axis damper along the wheel axes, and a steel bar web crossing the chassis interior in order to enhance the structure stiffness. The selected wheel bearing model for the first prototype required the use of several *ad-hoc* mechanical adapters, which increased the robot weight, cost and complexity.

For the next version, a new wheel bearing model will be used. The right-angle gearbox showed to be a good choice for the mechanical arrangement. Alternatively, we can use a straight-angle gearbox embedded in the wheel, which is a more compact solution. A more suitable and economic power/motor selection should be performed for the next version, because this was oversized for the first prototype, given that the power requirement scenario was still unknown. The robot width should be reduced so that the robot can fit between the sugarcane tunnels in higher plant scenarios, such as 3 meters tall tunnels. Finally, some original design features should be brought back, such as: aluminum carcass walls - in order to reduce the weight and power demand - and belts/pulleys in place of chains and sprockets - in order to reduce noise and backlash.

4.2 Improvement of Embedded Electronics

The embedded electronics system showed to be robust to vibrations and impacts. However, its main components were also oversized for the first prototype in terms of power and processing capacity. Planning the cost reduction for the next robot version, the computer should be replaced

by a more inexpensive solution, such as a Raspberry Pi 3. The VSS system will be composed of a customized printed circuit board (PCB) based on ATMEL AVR microcontrollers, which will replace the Arduino, the current device power connections and many wiring. This will better organize the power distribution and enlarge the possibilities of communication, integration of new sensors, and programming. Originally, the idea of using solar photovoltaic (PV) panels for the power supply was being studied. However, for the current design, they became unrealistic, if we consider the technology efficiency limitations and the robot dimensional design constraints.

In future developments close to the available commercial version, the robot can have significantly weight reduction and more efficient power drivers. This can bring, together with possible and notable advances in Solar PV technology, the possibility of re-including this in the robot design and giving to it the expected power autonomy.

4.3 Software, Control and Navigation

The software architecture should go through several implementations in order to provide the expected features for the next robot versions, such as: trajectory control, navigation, communication of computer with the VSS/self-monitoring, and autonomy. The trajectory control is the first step for the implementation of the robot autonomy, since it should be able to follow a predefined path along the sugarcane tunnel. For the navigation through the tunnels, different techniques based on the available sensors are being investigated, such as: following a corridor of points generation by the laser scanner mapping, following a path defined by the thermal mapping, and using GPS/IMU to follow a path of known points with predefined GPS geographic coordinates, which are given by UMOE BioEnergy. The combination of those methods together with robot mapping techniques may boost the definition of an efficient and low-cost solution for the robot navigation.

4.4 New Features

During the farm visit, some demand for new features were investigated, being the collection of sugarcane samples and pest control the most remarkable. The sampling is a frequent procedure performed in the UMOE BioEnergy fields, which aims to detect pests in the sugarcane. This is a tedious procedure subjected to extreme weather, since the company staff may need to travel a long distance to the desired sampling point within the farm area, infiltrate the sugarcane tunnels and slice lengthwise or crosswise one piece of the sugarcane stem (Fig. 15a).

For the next robot version, one possible solution for this problem is to attach a low-cost

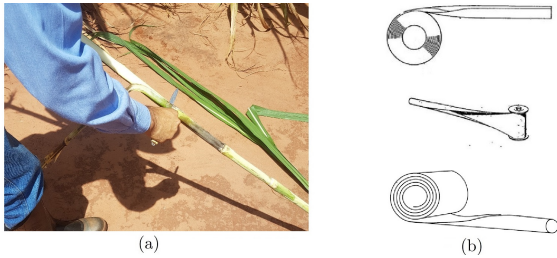


Figure 15: Sugarcane sampling in UMOE BioEnergy fields - (a) current procedure, the stem should be sliced or cut crosswise; (b) STEM, a compact solution for a lightweight sampling arm.

lightweight robotic arm on the robot chassis. Since this is a simple and low-payload task, there is no need of a complex structure with several degrees-of-freedom. An interesting solution to be investigated is a serial manipulator formed by multiple Storable Tubular Extendible Members (STEM[®], U.S. patents 3,144,215 and 3,434,674), which are measure tapes that extend as prismatic joints and retracts inside their chambers in a compact solution, as shown in Fig. 15b. Few studies about this structure can be found in the literature, such as (Seriani and Gallina, 2015). Finally, the pest control is a required feature to overcome the frequent problem of pest incidence. Some approaches for pest detection are being investigated, such as a drone for capturing aerial images with the Normalized Difference Vegetation Index (NDVI) applied. The collected images of the same sugarcane field at UMOE BioEnergy farm showed to be promising to detect the location of pest and send the robot directly to those points for a precise application of the pest control substance.

References

- Bac, C. W., van Henten, E. J., Hemming, J. and Edan, Y. (2014). Harvesting Robots for High-value Crops: State-of-the-art Review and Challenges Ahead, *Journal of Field Robotics* **31**(6): 888–911.
- Bechar, A. and Vigneault, C. (2017). Agricultural Robots for Field Operations. Part 2: Operations and Systems, *Biosystems Engineering* **153**: 110–128.
- Billingsley, J., Visala, A. and Dunn, M. (2008). Robotics in Agriculture and Forestry, in B. Siciliano and O. Khatib (eds), *Springer Handbook of Robotics*, Springer Berlin Heidelberg, pp. 1065–1077.
- Davis, R. J., Baillie, C. P. and Schmidt, E. J. (2009). Precision Agriculture Technologies - Relevance and Application to Sugarcane Production, *The 2009 CIGR Int. Symp. of the Australian Soc. for Eng. in Agriculture*.
- Edan, Y., Han, S. and Kondo, N. (2009). Automation in Agriculture, in S. Y. Nof (ed.), *Springer Handbook of Automation*, Springer-Verlag Berlin Heidelberg, pp. 1095–1128.
- Fehlman, W. L. and Hinders, M. K. (2009). *Mobile Robot Navigation with Intelligent Infrared Image Interpretation*, Springer Science & Business Media.
- Grimstad, L. and From, P. J. (2017). Thorvald II - a Modular and Re-configurable Agricultural Robot, *Proc. of the 20th IFAC World Congress*, Toulouse, France, pp. 4588–4593.
- Lambert, A., Furgale, P., Barfoot, T. D. and Enright, J. (2011). Visual Odometry Aided by a Sun Sensor and Inclinometer, *IEEE Aero. Conf.*, Big Sky, MT, USA, pp. 1–14.
- Li, L., Zhang, Q. and Huang, D. (2014). A Review of Imaging Techniques for Plant Phenotyping, *Sensors* **14**(11): 20078–20111.
- Midtiby, H. S., Åstrand, B., Jørgensen, O. and Jørgensen, R. N. (2016). Upper Limit for Context-based Crop Classification in Robotic Weeding Applications, *Biosystems Engineering* **146**: 183–192.
- Ortega, P., López-Rodríguez, G., Ricart, J., Domínguez, M., Castañer, L. M., Quero, J. M., Tarrida, C. L., García, J., Reina, M., Gras, A. et al. (2010). A Miniaturized Two Axis Sun Sensor for Attitude Control of Nano-Satellites, *IEEE Sensors Journal* **10**(10): 1623–1632.
- Quigley, M., Conley, K., Gerkey, B., Faust, J., Foote, T., Leibs, J., Wheeler, R. and Ng, A. Y. (2009). ROS: an open-source Robot Operating System, *Proc. of the ICRA Workshop on Open Source Software*.
- Seriani, S. and Gallina, P. (2015). A Storable Tubular Extendible Member (stem) Parallel Robot: Modelization and Evaluation, *Mechanism and Machine Theory* **90**: 95–107.
- SolarMEMS (2017). *Solar MEMS Technologies S.L. - Sun Sensor NANO-ISSX/c - Technical Specifications*, 1.04 edn.
- Tchoń, K., Zadarnowska, K., Arent, K. et al. (2015). Modeling and Control of a Skid-steering Mobile Platform with Coupled Side Wheels, *Bulletin of the Polish Academy of Sciences Technical Sciences* **63**(3): 807–818.

Volpe, R. (1999). Mars Rover Navigation Results using Sun Sensor Heading Determination, *IEEE/RSJ Int. Conf. on Intell. Rob. and Syste.*, Vol. 1, pp. 460–467.

Wong, J. Y. (2008). *Theory of Ground Vehicles*, 4th edn, John Wiley & Sons, Inc.